

# Soil Microbial Functional Succession Over One Year of Human Decomposition

Allison R. Mason<sup>1</sup>, Lois S. Taylor<sup>2</sup>, Naomi E. Gilbert<sup>1</sup>,  
Steven W. Wilhelm<sup>1</sup>, Jennifer M. DeBruyn<sup>1,2\*</sup>

<sup>1</sup>Department of Microbiology, University of Tennessee-Knoxville, 1311  
Cumberland Avenue, Knoxville, 37996.

<sup>2</sup>Department of Biosystems Engineering and Soil Science, University of  
Tennessee-Knoxville, 2506 E.J. Chapman Drive, Knoxville, 37996.

\*Corresponding author(s). E-mail(s): [jdebruyn@utk.edu](mailto:jdebruyn@utk.edu);

## Abstract

During terrestrial vertebrate decomposition, host and environmental microbial communities work together to drive biogeochemical cycling of carbon and nutrients. These mixed communities undergo dramatic restructuring in the resulting decomposition hotspots. To reveal the succession of both the active microbial members and the metabolic pathways they use, we generated metatranscriptomes from soil samples collected over one year from below three decomposing human bodies. Soil microbes increased expression of “heat shock” proteins in response to decomposition products changing physiochemical conditions (*i.e.*, reduced oxygen, high salt). Increased fungal lipase expression implicated fungi as key decomposers of fat tissue. Expression of nitrogen cycling genes was phased with soil oxygen concentrations: during hypoxic soil conditions, genes catalyzing N-reducing processes (*e.g.*, hydroxylamine to nitric oxide and nitrous oxide to nitrogen gas during reduced oxygen conditions) were increased, followed by increased expression of nitrification genes once oxygen diffused back into the soil. Increased expression of bile salt hydrolases implicated a microbial source for

the high concentrations of taurine typically observed during vertebrate decomposition. Collectively, microbial gene expression profiles remained altered even after one year. Together, we show how human decomposition alters soil microbial gene expression, revealing both ephemeral and lasting effects on soil microbial communities.

**Keywords:** Human Decomposition, Microbial Succession, Metatranscriptomics, Soil Microbial Ecology

## Introduction

Soil microbial communities are important drivers of ecosystem processes in terrestrial environments. Many soil microbes are decomposers that degrade complex organic matter and drive nutrient cycling in terrestrial ecosystems. Environmental disturbances can impact the presence and/or activity of soil microorganisms involved in these cycles, ultimately affecting nutrient availability and greenhouse gas emissions, such as CO<sub>2</sub> and N<sub>2</sub>O [1, 2]. Vertebrate death and subsequent carcass deposition in terrestrial ecosystems is one disturbance resulting in the deposition of large quantities of organic C and N [3–10], along with other elements (P, K, S, *etc*) [11], which collectively contribute to microbially-mediated biogeochemical cycling. In addition to this, changes in pH, temperature, and fluctuations in soil oxygen provide abiotic filtering further impacting microbial metabolic strategies [7–9, 11–13]. Vertebrate decomposition also results in mixing of host and environmental microbes: the animal’s microflora are flushed into the soil along with decomposition products where they further contribute to decomposition processes (*e.g.*, organic nitrogen mineralization) [14].

While C and N transformations have been documented during decomposition, the functional response of microbes and their roles in nutrient cycles remain unclear. The composition and structure of decomposition-impacted soil microbial communities have been investigated using sequencing of marker genes amplicons (*i.e.*, 16S rRNA, 18S

rRNA, ITS). This has allowed for the identification of changes in microbial biodiversity and taxonomic succession in response to vertebrate decomposition, revealing patterns that include increases in the anaerobic taxa *Firmicutes* and *Bacteroidetes* [15]. However, few studies have integrated soil biogeochemistry with microbial community composition, which can further help to describe microbial ecology in these decomposition systems. Taylor et al. (2024) [13] showed that fungal community shifts were linked to changes in soil dissolved oxygen, highlighting interactions between soil microbes and changes in the surrounding environment. While insightful for making potential connections between taxa and environment, these analyses do not inform which taxa are active members of the community, which functional pathways/genes are expressed, and how these pathways facilitate decomposition processes.

RNA sequencing (*i.e.*, metatranscriptomics) and metabolomics can be used to investigate microbial community functional succession during decomposition. They can identify how ecological functions, including C and N cycling, are impacted by decomposition events in terrestrial ecosystems. To date, applications of metatranscriptomics to vertebrate decomposition samples have been limited to internal host communities [16, 17]: Burcham et al. (2019) [16] revealed differential expression of amino acid and carbohydrate metabolism in the heart during mouse decomposition, while Ashe et al. (2021) [17] documented taxonomic shifts in gene expression of oral microbial communities during human decomposition.

We expected that the impacted soil microbial community, which includes a mix of host and environmental taxa, would also have altered gene expression profiles, given the release of decomposition byproducts into the soil during terrestrial decomposition. We previously assessed the decomposition-impacted soil metabolome [18], demonstrating a prevalence of amino acids and suggesting upregulation of organic nitrogen metabolic pathways. Additionally, DeBruyn et al. (2021) [18] showed the soil metabolome was

139 surprisingly still altered compared to starting conditions at the end of that 21-week  
 140 study, suggesting long-term impacts of decomposition on soil microbial functioning.  
 141  
 142 Here, we investigated soil microbial gene expression during a one-year period of human  
 143 decomposition. The overarching goal of this work was to assess the effects of vertebrate  
 144 decomposition on ecosystem function by characterizing community-level shifts in soil  
 145 microbial function. We hypothesized that: (i) gene expression would shift over time as  
 146 resources were consumed and transformed and soil chemical and physical conditions  
 147 changed due to the influx of decomposition products during soft tissue degradation  
 148 [8, 9, 18]; (ii) gene expression for enzymes involved in nitrogen cycling would be  
 149 altered, as changes in nitrogen pools have been previously described in decomposition  
 150 soils [8]; (iii) expression of genes involved in lipid metabolism would increase, as lipids  
 151 from the body entered the soil during decomposition and previous studies identified  
 152 lipolytic organisms in decomposition soils [12, 19]; (iv) microbial expression profiles  
 153 in the impacted soil would remain altered even after a year, as previous studies have  
 154 shown that community composition [20, 21] can remain altered longer than a year.  
 155 We analyzed metatranscriptomes of soil samples collected at six key timepoints over  
 156 one year of human decomposition to determine the identity of active populations and  
 157 the expression of genes and pathways relevant to the enhanced biogeochemical cycling  
 158 observed in decomposition hotspots. We compared gene expression between decom-  
 159 position timepoints and control soils that were unexposed to decomposition products  
 160 to identify functions or functional pathways of interest. We show: (i) decomposition  
 161 shifts soil microbial community gene expression, with the effects still measurable after  
 162 one year; (ii) expression of genes related to stress response are elevated in decompo-  
 163 sition soils; (iii) expression of genes encoding triacylglycerol lipase differed between  
 164 fungi (increased) and bacteria (decreased); (iv) evidence for phased nitrification and  
 165 denitrification, driven by changes in soil dissolved oxygen; (v) evidence for organic  
 166  
 167  
 168  
 169  
 170  
 171  
 172  
 173  
 174  
 175  
 176  
 177  
 178  
 179  
 180  
 181  
 182  
 183  
 184

sulfur processing (taurine) via bile salt hydrolases. This direct assessment of function expands the fundamental understanding of terrestrial vertebrate decomposition, providing insight into pathways of biogeochemical cycling within these hotspots.

## Results

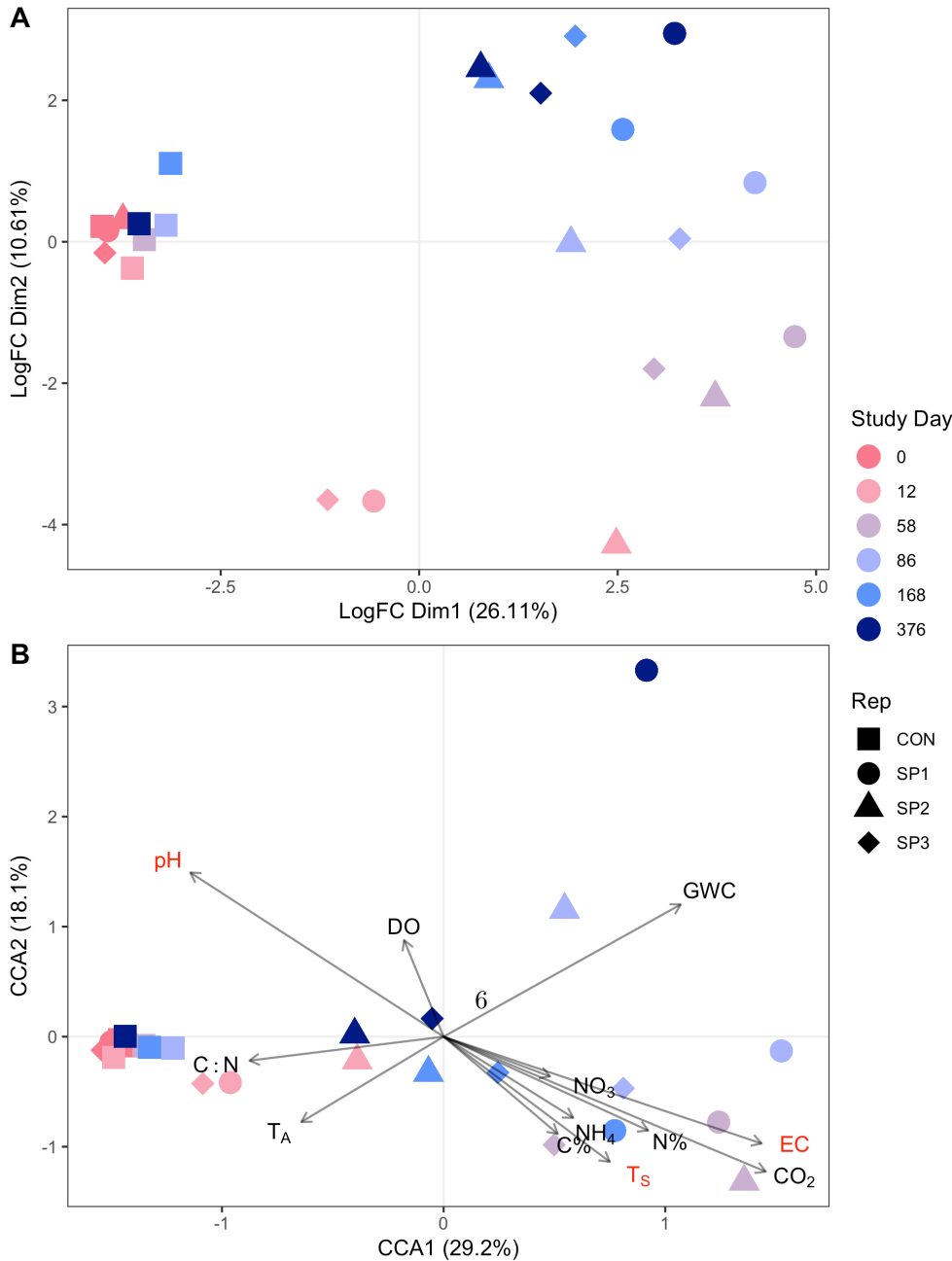
### Soil Physiochemistry

Soil chemistry was altered in response to the presence of a decomposing human cadaver, with multiple parameters still impacted after one year [13]. Generally, soil pH decreased and remained low in decomposition soils of all but one individual. Soil electrical conductivity (EC) increased in response to decomposition, remaining elevated through approximately day 58 before gradually decreasing throughout the remainder of the study (Supplementary Material 1). Respiration (evolved CO<sub>2</sub>) increased by an order of magnitude beginning at day 12, which corresponded to a reduction in soil dissolved oxygen (DO) to 29% - 48.9%. Ammonium concentrations increased 78-fold, reaching maximum concentrations between days 12 and 58. This was followed by decreased ammonium and increased nitrate concentrations at day 86, with nitrate concentrations reaching a maximum at day 168 (Supplementary Material 1).

### Microbial gene expression in response to human decomposition

Gene expression profiles in decomposition-impacted soils shifted away from controls and day zero samples as decomposition progressed (Fig 1A). Expression was most different from controls on study days 58, 86, 168 (Supplementary Material 2), before returning toward control conditions on study day 376. After one year of decomposition, soil gene expression profiles had not returned to pre-decomposition conditions, as evidenced by their clustering away from controls and day zero samples in the MDS plot (Fig 1A).

**Figure 1: Microbial gene expression profiles are altered during human decomposition.** Multidimensional scaling (MDS) shows gene expression within soils changed as decomposition progressed (A). Additionally, canonical correspondence analysis (CCA) shows that environmental variables explained 47.3% of the variation in gene expression profiles (B). Variables in bold red type significantly ( $p < 0.05$ ) explained some of the variation in gene expression profiles as assessed by Permutational Analysis of Variance (PERMANOVA). In both panels soils from controls (CON) and the three donors (SP1, SP2, SP3) are denoted by symbol shape, while color represents study day. In B, soil physiochemical variable loadings are represented by arrows: Gravimetric water content (GWC), electrical conductivity (EC), pH (pH), dissolved oxygen (DO), respiration (evolved  $\text{CO}_2$   $\mu\text{mol gdw}^{-1}$ ), ammonium ( $\text{NH}_4$ ), and nitrate ( $\text{NO}_3$ ) concentrations ( $\text{mg gdw}^{-1}$ ), percent carbon (%C), percent nitrogen (%N), carbon:nitrogen ratio (C:N), ambient temperature ( $T_A$ ), and soil temperature ( $T_S$ ).



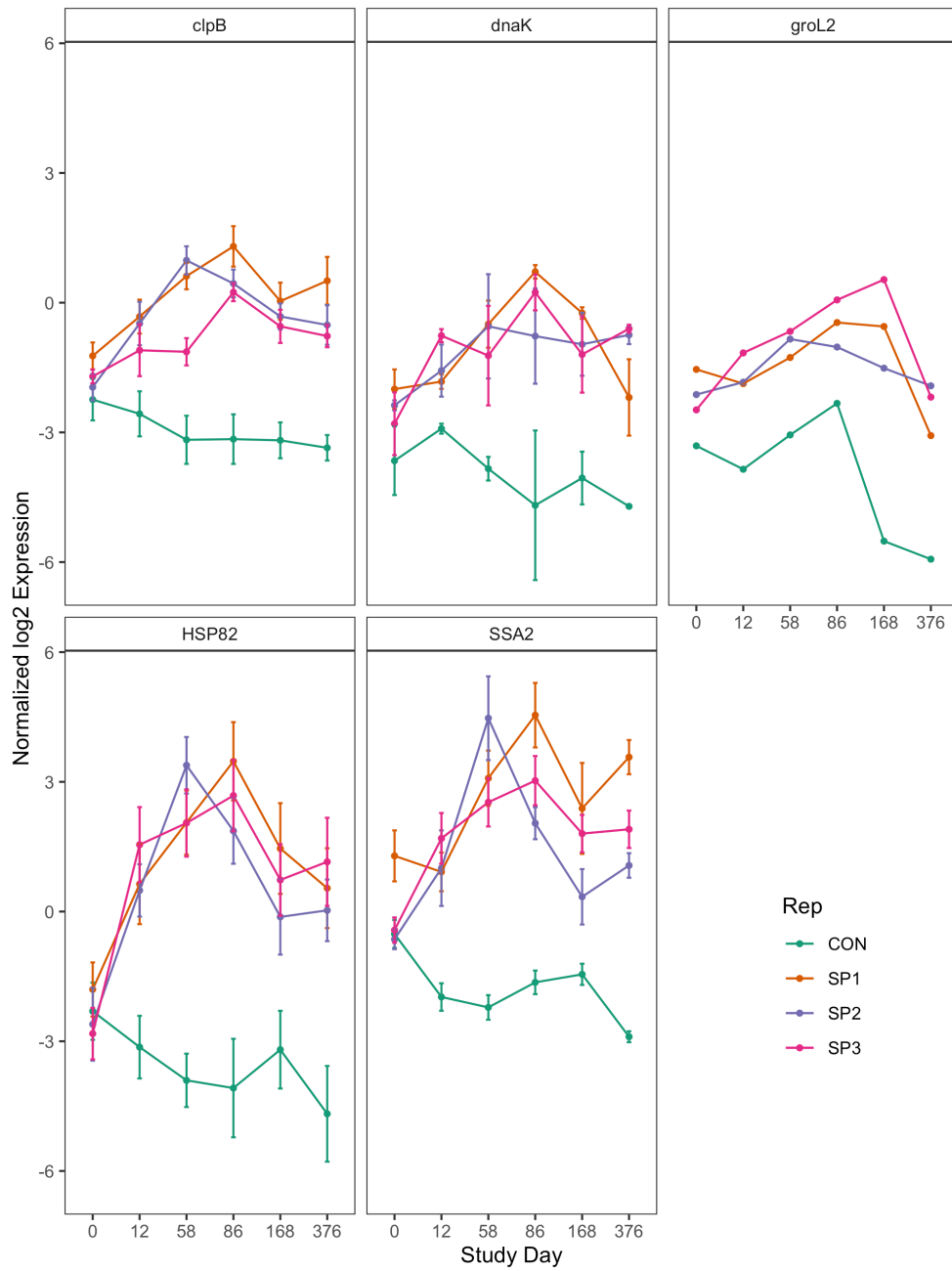
Some correlations were observed between gene expression shifts and soil physiochemical data at decomposition timepoints. Canonical correspondence analysis (CCA) was used to constrain gene expression data with soil physiochemical data (Fig 1B). CCA1 and CCA2 explained 29.2% and 18.1% of the variance in gene expression, respectively. Transcript profiles at day 12 were associated with an increase in soil carbon to nitrogen ratio (C:N). Gene expression profiles at days 58 to 86 were positively correlated with increased soil temperature, EC, and evolved CO<sub>2</sub>, while study day 168 was associated with elevated levels of soil NO<sub>3</sub>. Further, Permutational Analysis of Variance (PERMANOVA) revealed that internal accumulated degree hours (ADH) ( $p = 0.001$ ), soil temperature ( $p = 0.039$ ), pH ( $p = 0.033$ ), and EC ( $p = 0.031$ ) significantly explained some of the variation in gene expression profiles ( $p < 0.05$ ). No other soil chemical variables were significant at  $\alpha = 0.05$  (Supplementary Material 3).

Overall, decomposition changed soil gene expression profiles over the one-year study relative to control soils. Differential expression analysis between decomposition and control soils identified 7,047 down-regulated and 38,425 up-regulated genes. Gene transcripts that were associated with control soils belonged to a wide variety of clusters of orthologous genes (COG) functional categories. Specifically, the top 20 genes whose expression was higher in control soils belonged to ten unique COG categories, including signal transduction mechanisms, transcription, and those of unknown function. In contrast, the top 20 genes whose expression was higher in decomposition soils only fell into four COG categories (Supplementary Material 4 A): 1) post-translational modification, protein turnover, and chaperones; 2) energy production and conversion; 3) cell motility; and 4) carbohydrate transport and metabolism. The most common COG category represented in decomposition soils (80% of the top 20 genes) was post-translational modification, protein turnover, and chaperones. Within this category, several heat shock stress response genes were identified, including clpB, dnaK, groL2, SSA2, HSP82, and clpB (Supplementary Material 5). Further investigation of these

genes over time shows that their expression increased, typically reaching maximum transcript levels around study days 58 and 86 (Fig 2). This corresponded to elevated soil temperatures below decomposing bodies between study days 12-80, with soil temperatures increasing to approximately 43°C [13], as well as maximum soil EC and minimum dissolved oxygen measurements between days 12 and 58 (Supplementary Material 1).

**Figure 2: Mean normalized log2 expression of heat shock proteins identified by differential expression analysis comparing decomposition and control soils.** Each panel represents a single heat shock gene, labeled with gene names, identified via Prodigal. Symbol color denotes if the sample is a control (CON, green), or one of three individuals: SP1 (orange), SP2 (purple), or SP3 (pink). Error bars are standard error of individual query genes in the top 20 transcripts associated with decomposition soils.





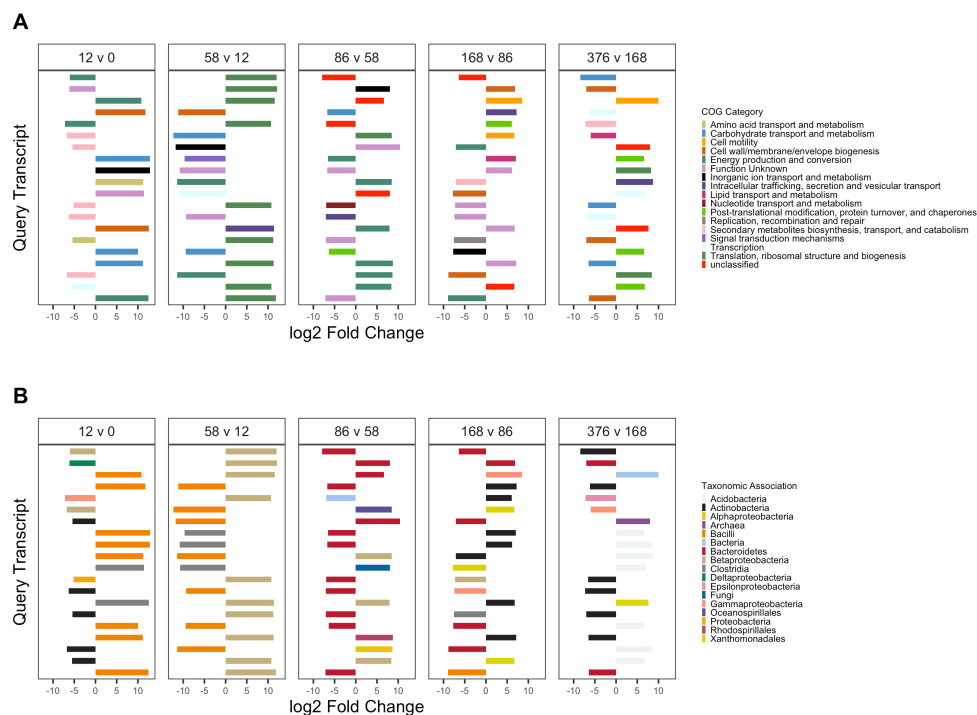
Taxonomy associated with top differentially expressed gene transcripts also differed between control and decomposition soils. The top 40 significantly differentially

expressed gene transcripts in decomposition soils were associated with Fungi, *Actinobacteria*, and *Xanthomonadales*, while gene transcripts in controls were associated with *Acidobacteria*, *Cyanobacteria*, *Proteobacteria* ( $\alpha$ ,  $\delta$ ,  $\gamma$ ), and *Planctomycetes* (Supplementary Material 4 B). The greatest number of differentially expressed genes relative to control samples was observed at day 86, where we saw 145,460 and 124,883 up- and down-regulated genes, respectively.

## Temporal gene expression shows shifted in decomposer functions

Differential expression analysis between sequential study days revealed which genes were altered during decomposition time. The top ten significantly up- and down-regulated genes, determined by the lowest p-values from differential expression analysis (cutoff =  $\alpha < 0.05$ ), are reported in Supplementary Material 6 and Fig 3.

**Figure 3: Top twenty up- and down-regulated genes in decomposition soils comparing sequential study days (0, 12, 58, 86, 168, 376) colored by COG functional category (A) and taxonomic annotation (B).** Positive values denote increased expression compared to the preceding timepoint, while negative values denote a decrease.



Expression of genes annotated with the COG categories cell wall/membrane/envelope biogenesis, inorganic ion transport and metabolism, and carbohydrate transport and metabolism increased proportionally from day 0 to 12. In contrast, expression of secondary metabolite biosynthesis, transport, and catabolism genes decreased during this period (Fig 3A). Transcripts from *Bacilli* and *Clostridia* increased, while transcripts from *Actinobacteria* decreased between study days zero and 12 (Fig 3).

Between days 12 and 58, 90% of the top 10 upregulated genes were associated with the translation, ribosomal structure and biogenesis COG and all were taxonomically associated with *Betaproteobacteria* (Fig 3A,B). Many of these genes were annotated as ribosomal protein large (RPL), involved in ribosomal binding. Genes across multiple COG categories with taxonomic associations to *Bacilli* and *Clostridia* decreased

507 between study days 12 and 58, six of which were transcripts that previously increased  
508  
509 between days zero and 12 (Fig 3B, Supplementary Material 6).

510

511 Multiple transcripts associated with the energy production and conversion COG, as  
512 well as transcripts annotated with the COGs inorganic transport and metabolism,  
513 and translation, ribosomal structure and biogenesis, increased between days 58 and  
514 86 (Fig 3A). Two of the upregulated energy and production and conservation tran-  
515  
516 scripts were associated with cytochrome c oxidase subunits in *Betaproteobacteria*,  
517  
518 while another was annotated as *hao*, encoding the enzyme hydroxylamine dehydroge-  
519  
520 nase which is involved in conversion of hydroxylamine to nitrite during nitrification  
521  
522 (Supplementary Material 6). Further investigation into hydroxylamine dehydrogenase  
523  
524 showed a significant increase in *hao* transcripts at day 86 followed by subsequent  
525  
526 decreases at days 168 and 376 ( $F = 4.183$ ;  $p = 0.02$ ). This increase corresponded to  
527  
528 decreased soil ammonium levels and subsequent accumulation of nitrate (Supplemen-  
529  
530 tary Material 1). Half of the topmost downregulated genes between days 58 and 86  
531  
532 were not assigned to a COG (*i.e.*, unclassified) or were of unknown function.

533

534 Differential expression comparing study days 86 with 168 and 168 with 376 identified  
535  
536 genes across a variety of functional categories, with many unclassified in the COG  
537  
538 database or with unknown function (Fig 3A). Expression of carbohydrate transport  
539  
540 and metabolism genes associated with *Bacilli* decreased between day 168 and 376.  
541  
542 *Acidobacteria* transcripts increased in decomposition-impacted soils between study  
543  
544 day 168 and 376, but were not associated with any single COG category (Fig 3B).

545

## 546 **Organic carbon metabolism**

547

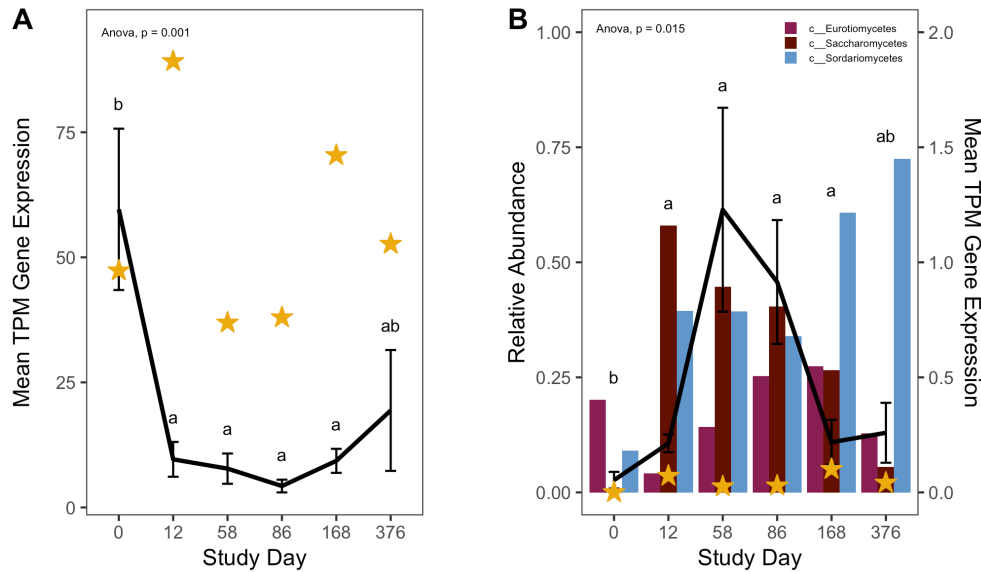
548 We expected to observe increased expression of lipid metabolizing genes during active  
549  
550 and advanced decomposition as microbes degraded lipids deposited in the soil [19].

551

552

Therefore, we investigated changes in triacylglycerol lipase (enzyme commission number: 3.1.1.3) gene transcription in our soils. Generally, lipase transcripts decreased as decomposition progressed (HLM  $F = 6.564$ ,  $p < 0.001$ ), however we also observed a significant interaction between study day and taxonomic annotation ( $F = 8.786$ ;  $p < 0.001$ ). Specifically, lipase gene transcripts annotated as bacteria decreased with decomposition time ( $F = 10.392$ ;  $p = 0.001$ ), while fungal lipase transcripts increased, reaching a maximum at study day 58 ( $F = 4.509$ ;  $p = 0.015$ ) (Fig 4).

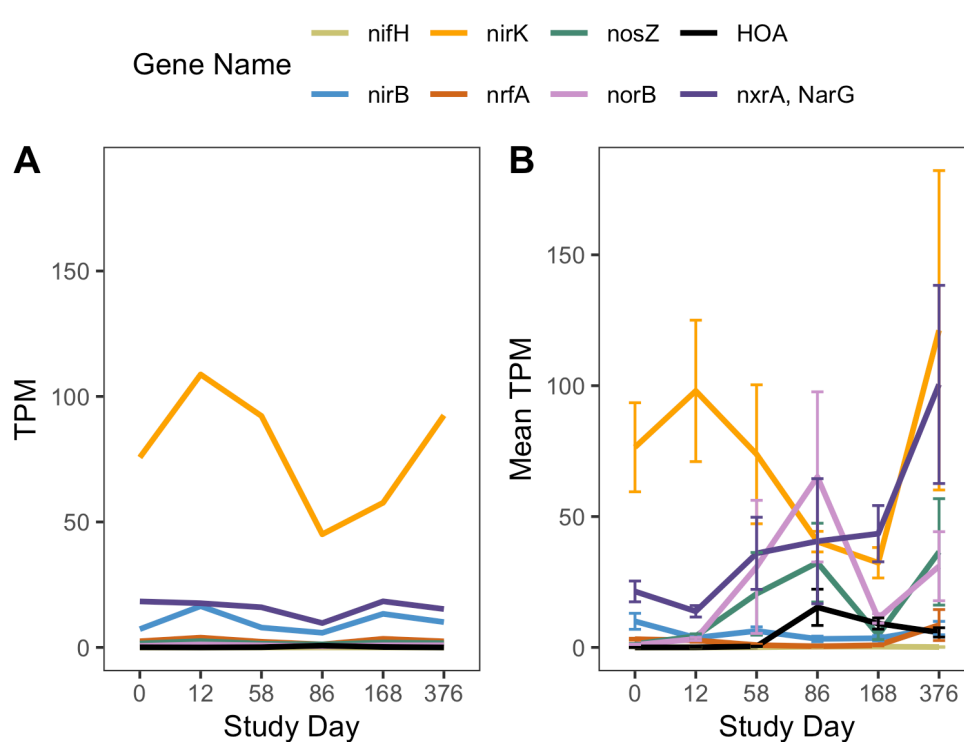
**Figure 4: Mean transcript abundance, in transcripts per million (TPM), of all bacterial (A) and fungal (B) triacylglycerol lipase (EC 3.1.1.3) genes over time.** Black lines (A, B) report mean and standard deviation of TPM from three individuals (black line), while gold stars denote mean TPM in control soils. P-values are the result of ANOVAs where average TPM and study day are the dependent and independent variables, respectively, while letters are the result of post-hoc Tukey tests between decomposition timepoints. In B, bars show the relative abundance of the fungal classes *Saccharomycetes*, *Sordariomycetes*, and *Eurotiomycetes*, reported in Taylor et al. (2024).



## Nitrogen- and sulfur compound transformations

Expression of nitrogen cycling genes was impacted in response to human decomposition. Due to the detection of hydroxylamine oxidoreductase (*hao*) transcripts in our differential expression analysis, and our hypotheses predicting changes to nitrogen transformation processes, the expression of genes encoding common enzymes involved in nitrogen cycling (*nifH*, *nirB*, *nirK*, *norB*, *nosZ*, *nrfA*, *nxrA*, and *amoA*) were assessed using their enzyme commission numbers (Fig 5A,B). *nifH*, encoding a subunit of nitrogenase which is involved in nitrogen fixation, displayed little to no changes in gene expression between control and decomposition soils. Transcripts for two genes encoding enzymes contributing to the last two steps of denitrification, *norB* (nitric oxide reductase) and *nosZ* (nitrous oxide reductase), increased between study days 12 and 86, and decreased at study day 168 before increasing again at day 376. In contrast, expression of genes encoding nitrate reductase, *narG*, and NO-forming nitrite reductase, *nirK*, remained low until day 376 when transcripts for both genes increased. As noted above, expression of *hao*, encoding hydroxylamine dehydrogenase, increased at study day 86 before decreasing at remaining timepoints (Fig 3A, Fig 5B). Expression of *amoA*, encoding a subunit of ammonia monooxygenase, and *nxrA*, encoding a subunit of nitrite oxidoreductase, which are involved in nitrification, changed in response to decomposition. *amoA* transcripts initially decreased at day 12, remaining reduced until study day 376. Similarly, abundance of genes that encode for enzymes involved in dissimilatory nitrate reduction, *nirB*, and *nrfA*, was low for the first 168 days, with *nrfA* expression increasing at day 376 (Fig 5B).

**Figure 5: Mean gene expression, in transcripts per million (TPM), of commonly used marker genes for enzymes involved in nitrogen cycling over time in controls (A) and decomposition (B) soils.** Data in B represent mean and standard deviation of TPM from three individuals.

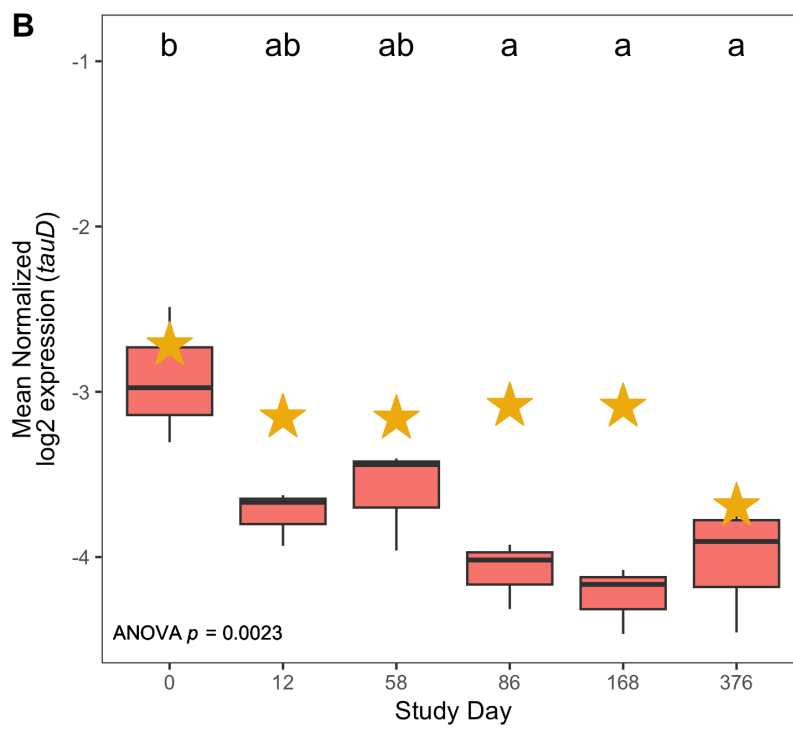
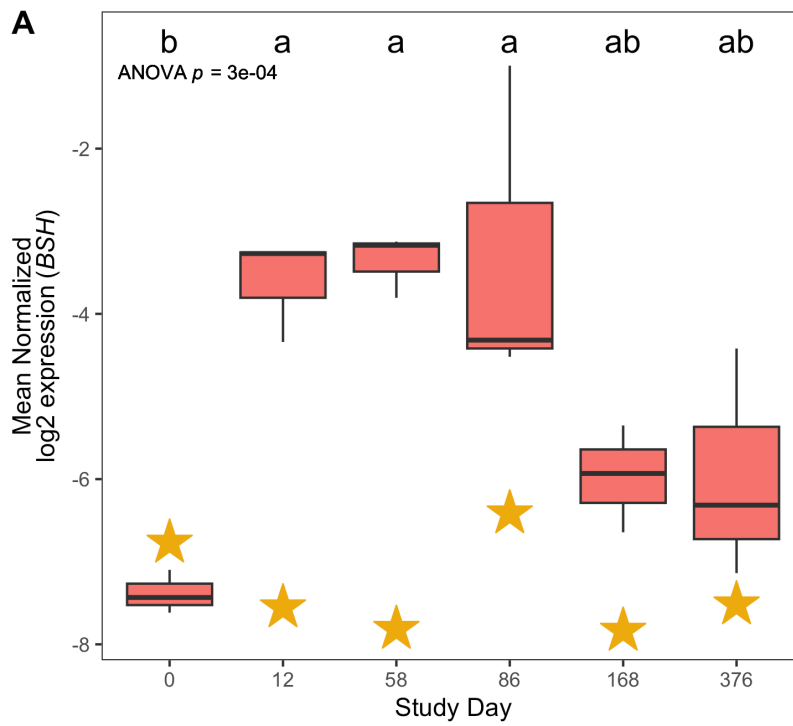


Expression of genes involved in metabolism of nitrogen and sulfur-containing compounds were also impacted by human decomposition. Specifically, four of the top ten genes whose expression decreased at day 12 were related to taurine metabolism, with their annotations associated with *tauD*, encoding taurine dioxygenase. (Supplementary Material 6). Further investigation into *tauD* showed that mean expression of these genes decreased steadily over one year, beginning at day 12 (Fig 6B); however, *tauD* expression in response to human decomposition was variable across taxonomic associations. Most *tauD* transcripts were associated with *Gammaproteobacteria*, *Actinobacteria*, *Betaproteobacteria*, *Alphaproteobacteria*, and fungi. While a majority of the *tauD* gene queries displayed reduced expression over time, expression of fungal-associated and a few *Betaproteobacteria*-associated *tauD* genes increased at day 58 (Supplementary Material 7). Sources of taurine in the human body include taurine

absorbed from the diet and taurine produced from anaerobic microbial deconjugation of bile salts via bile salt hydrolase (BSH) enzymes [22]. Therefore, we examined expression for genes encoding BSH enzymes in decomposition soils. Expression of these genes was elevated at days 12, 58, and 86 before converging toward pre-decomposition levels at days 168 and 376 (Fig 6A). Hierarchical linear mixed effects (HLM) models showed that both *tauD* (HLM  $F = 7.356$ ,  $p = 0.002$ ) and BSH ( $F = 13.768$ ,  $p < 0.001$ ) gene expression was significantly different over time (Fig 6A,B).

**Figure 6: Mean bile salt hydrolase, BSH, (A) and *tauD*, taurine dioxygenase, (B) log2 normalized expression in controls (gold stars) and decomposition (boxplots) soils.** Boxplots display the 25th and 75th quartiles and median log2 normalized values between all three individuals at each timepoint. ANOVA p-value is the result of a hierarchical linear mixed effects model accounting for repeated measures of each donor block, while letters denote the results of *post-hoc* Tukey test.





## Discussion

The goal of this study was to assess microbial gene expression in soils responding to human decomposition. Metatranscriptomics were applied to soil samples collected over one year from below three decomposing human bodies. From this, we found that microbial gene expression reproducibly shifted over time. Additionally, we showed that gene expression profiles had not recovered to pre-decomposition conditions after one year. Comparison of control and decomposition expression profiles revealed that heat-shock proteins were elevated in response to decomposition. We also described expression patterns between decomposition timepoints, noting changes in functional gene categories at certain timepoints, in particular with respect to lipid, nitrogen and sulfur metabolism.

### Decomposition impacted soil community gene expression, for at least one year

Gene expression profiles remained altered after one year of decomposition. It is unclear if soil microbial communities, in terms of gene expression profiles, have reached a new steady state as a result of decomposition, or if they would eventually return to pre-decomposition conditions. The soil pH, EC,  $\text{NH}_4^+$ ,  $\text{NO}_3^-$ , and total nitrogen (TN) exhibited differences (although not statistically significant) in these soils following a year of decomposition, however bacterial and fungal community structures, as assessed by rRNA amplicon libraries, were still altered [13]. This indicates that decomposition can continue to structure microbial communities and impact their function for extended periods of time. While nutrient pools and communities both demonstrate less rapid change at later time points in the study, there is no evidence suggesting an arrival at a steady-state post-disturbance microbial community within our study. In some studies, human decomposition can result in elevated carbon and nutrients (organic nitrogen, ammonium, nitrate, and phosphate) for longer than a year [3], suggesting

decomposition events have long-lasting effects on the local ecosystem. Together, this has implications for terrestrial ecosystem processing (*e.g.*, nutrient cycling, emission of greenhouse gasses, etc.), as we show that decomposition alters functional metabolism pathways within soil microbial communities. It is clear that extended sample collections beyond a single year are needed to address how long microbial communities are effected, and whether there is a return to the original state or some new altered community condition.

Bacteria, fungi, and archaea were all represented by expressed genes throughout decomposition, suggesting that members of all three domains have the potential to contribute to decomposition processes and nutrient cycling. While a majority of annotated transcripts were identified as bacterial, fungal transcripts were the second most abundant group. Fungal transcripts made up almost half (*e.g.*, seven of the top fifteen) of the significantly differentially expressed genes associated with decomposition-impacted soils. Additionally, with respect to expression shifts between decomposition timepoints, fungal transcripts were among the topmost upregulated genes at study day 86. This is not surprising as fungi are key decomposers, involved in the degradation of organic matter in terrestrial ecosystems [23]. It was interesting to see an increase in certain fungal transcripts, such as lipase, at study days 58 and 86 when soil oxygen began to recover. We would expect lipids to enter the soil as tissues are broken down during decomposition, so we were surprised to see bacterial lipase genes decrease during decomposition. This suggests that microbial activity in decomposition soils may be constrained by the changing chemical environment, potentially altered oxygen levels in the case of bacterial lipase gene expression. Prior work with these same soils showed that soil oxygen concentration was a key driver of changes in both bacterial and fungal community composition [13].

## 875 Increased stress responses during decomposition

876

877 Soil microbial communities expressed stress response genes in response to human  
878 decomposition. Differential expression analysis identified increased expression of mul-  
879 tiple heat shock proteins associated with the taxa *Xanthomonadales*, *Actinobacteria*,  
880 and fungi. Upon further investigation, expression of these genes increased through  
881 day 58 and remained high for the remainder of the year. Soil temperature was ele-  
882 vated relative to controls between study days 8 and 80, with maximum temperatures  
883 >40°C, while soil electrical conductivity increased up to 663  $\mu\text{S}/\text{cm}$  (16X higher than  
884 background) through day 58 before slowly decreasing through the remainder of the  
885 study. Soil electrical conductivity correlates with ionic strength and can be an indica-  
886 tor of increased salinity [24]. With regard to vertebrate decomposition, early elevated  
887 conductivity in impacted soils is attributable to sodium (Na), potassium (K), and  
888 ammonium ( $\text{NH}_4$ ) [8–11, 13]. As a result, we would expect these microbes to be experi-  
889 encing both heat and osmotic stress during this period. Prior work has observed  
890 increased heat shock gene expression during salt stress in paddy soils [25] and the  
891 presence of both heat and osmotic stress genes in desert soils along a salt gradient [26],  
892 suggesting saline conditions can alter the expression of heat and/or osmotic stress  
893 genes. In our study we observed the stress response within soil microbial communities  
894 was stimulated during human decomposition. At this time, however, it is unclear if  
895 expression of these genes is in response to heat stress alone, or in combination with  
896 osmotic stress.

900

901

902

903

904

905

906

907

908

909

910

911

912

913

914

915

916

917

918

919

920

921

922

923

924

925

926

927

928

929

930

931

932

933

934

935

936

937

938

939

940

941

942

943

944

945

946

947

948

949

950

951

952

953

954

955

956

957

958

959

960

961

962

963

964

965

966

967

968

969

970

971

972

973

974

975

976

977

978

979

980

981

982

983

984

985

986

987

988

989

990

991

992

993

994

995

996

997

998

999

1000

1001

1002

1003

1004

1005

1006

1007

1008

1009

1010

1011

1012

1013

1014

1015

1016

1017

1018

1019

1020

1021

1022

1023

1024

1025

1026

1027

1028

1029

1030

1031

1032

1033

1034

1035

1036

1037

1038

1039

1040

1041

1042

1043

1044

1045

1046

1047

1048

1049

1050

1051

1052

1053

1054

1055

1056

1057

1058

1059

1060

1061

1062

1063

1064

1065

1066

1067

1068

1069

1070

1071

1072

1073

1074

1075

1076

1077

1078

1079

1080

1081

1082

1083

1084

1085

1086

1087

1088

1089

1090

1091

1092

1093

1094

1095

1096

1097

1098

1099

1100

1101

1102

1103

1104

1105

1106

1107

1108

1109

1110

1111

1112

1113

1114

1115

1116

1117

1118

1119

1120

1121

1122

1123

1124

1125

1126

1127

1128

1129

1130

1131

1132

1133

1134

1135

1136

1137

1138

1139

1140

1141

1142

1143

1144

1145

1146

1147

1148

1149

1150

1151

1152

1153

1154

1155

1156

1157

1158

1159

1160

1161

1162

1163

1164

1165

1166

1167

1168

1169

1170

1171

1172

1173

1174

1175

1176

1177

1178

1179

1180

1181

1182

1183

1184

1185

1186

1187

1188

1189

1190

1191

1192

1193

1194

1195

1196

1197

1198

1199

1200

1201

1202

1203

1204

1205

1206

1207

1208

1209

1210

1211

1212

1213

to decomposition, and these shifts differed between bacterial and fungal transcripts. Specifically, bacterial triacylglycerol lipase transcripts decreased in response to decomposition, while fungal triacylglycerol lipase transcripts increased. Further, expression of these genes corresponded to changes in relative abundance of the fungal classes *Saccharomycetes*, *Sordariomycetes*, and *Eurotiomycetes* [13]. These fungi have been previously associated with decomposition soils [27, 28] and are known to contain triacylglycerol lipase genes in their genomes [29, 30], suggesting that they play a role in lipid degradation in decomposition soils.

Our observation of an overall decrease in triacylglycerol lipase transcripts contrasts with previous work by Howard et al. (2010) [19], who observed increased gene copy number of Group 1 lipase genes via qPCR during swine decomposition. Fatty acid composition differs in human compared to pig tissue [31], potentially altering the lipids profile available for microbes, leading to differences in decomposition products within the soil [18]. These products can then directly or indirectly alter community composition and/or activity of functional proteins via substrate availability or the chemical environment. Further, decomposition of humans and pigs resulted in increased pH in soils below pigs, and decreased pH below humans [18]. Altered pH and soil chemistry could result in a different functional potential and/or gene expression in decomposition-impacted soils. Many triacylglycerol lipases have a pH optimum that is neutral to basic [32–34], so cells may be decreasing expression under acidic conditions in human decomposition soils. Availability of lipid species and changes to pH may select for taxa that favor these substrates/pH conditions; for example, Mason et al. (2022) [12] suggested the abundance of the fungal taxa *Saccharomycetes* was related to antemortem BMI due to relative proportions of fat and muscle tissue.

## 967 Evidence for phased denitrification and nitrification

968  
969 The human body is a concentrated source of nitrogen that is released into the sur-  
970 rounding soil during decomposition. Expression of common marker genes for nitrogen  
971 cycling was altered in decomposition soil and suggested nitrogen transformations  
972 during human decomposition are driven by soil oxygen concentrations with hydroxy-  
973 lamine as an important intermediate. We observed low or reduced expression of the  
974 nitrification genes *nrrA* and *amoA* between days 12 and 86, during a period when  
975 oxygen was reduced to 39% - 85%. This was concomitant with an accumulation of  
976 ammonium, which reached a maximum on day 12, and low nitrate conditions indicat-  
977 ing that nitrification was inhibited. This period of reduced soil oxygen constraining  
978 nitrification was also described in a decomposition experiment with beaver carcasses  
979 Keenan et al. (2018) [8].  
980  
981  
982  
983  
984  
985  
986  
987

988 We observed increased gene expression for the enzyme hydroxylamine dehydrogenase  
989 (HAO) at day 86 while oxygen was reduced (~85%). This corresponded to simultane-  
990 ous increases in expression of genes encoding nitric oxide reductase (*norB*) and nitrous  
991 oxide reductase (*nosZ*). Traditionally HAO has been thought to process hydroxy-  
992 lamine to nitrite during nitrification, while NorB and NosZ are enzymes involved in  
993 the last two steps of denitrification converting nitric oxide (NO) to dinitrogen gas  
994 ( $N_2$ ). However, recent work suggested hydroxylamine can be converted to nitric oxide  
995 (NO), and can interact with multiple phases of the nitrogen cycle [35]. Even though  
996 *amoA* expression was shown to decrease during reduced oxygen conditions, *amoA* tran-  
997 scripts were still present and likely able to convert ammonium to hydroxylamine as  
998 soil oxygen was not completely depleted during decomposition. Additionally, a previ-  
999 ous study reported that the growth of the ammonia oxidizing bacteria *Nitrosomonas*  
1000 *europaea* under anoxic conditions lead to accumulation of hydroxylamine in a chemo-  
1001 stat bioreactor [36], suggesting anaerobic ammonium oxidation (anammox) may also  
1002 be occurring in decomposition soils. However, we did not observe increases in *nirK*  
1003  
1004  
1005  
1006  
1007  
1008  
1009  
1010  
1011  
1012

expression, which might suggest conversion of nitrite to NO for use in the anammox pathway. NO produced via HAO activity may be used for anammox in these soils; however, the role of hydroxylamine as an intermediate in anammox is still debated [35]. Therefore, our current hypothesis is that hydroxylamine accumulates under anaerobic conditions during decomposition, which can then be converted to NO by HAO. This NO would then be present for anaerobic denitrifying bacteria to convert to nitrous oxide (N<sub>2</sub>O) by NorB and finally to N<sub>2</sub> by NosZ. Keenan et al. (2018) [8] noted a brief increase in N<sub>2</sub>O emissions, which suggests denitrification was occurring during this phase of reduced soil oxygen concentrations.

As soils fully reoxygenated by day 168, we observed increased expression of genes encoding enzymes involved in aerobic nitrification, *amoA* and *nxrR*. Nitrification is an oxygen-dependent process which would convert accumulated ammonium to nitrate; the increase in nitrate concentrations may then serve as a substrate for denitrification. We observed increased expression of marker genes encoding all four enzymes in the complete dissimilatory denitrification pathway (*narG*, *nirK*, *norB*, and *nosZ*) at day 376. Increased expression of nitrification and denitrification marker genes is consistent with the accumulation of nitrite, nitrate, and N<sub>2</sub>O after oxygen is reintroduced to soils described in Keenan et al. (2018) [3, 8]. Together, gene expression patterns in our study provide further insight into nitrogen transformations in during vertebrate decomposition, suggesting an important role of hydroxylamine.

## Increased expression of bile salt hydrolases

Sulfur is present in various organic molecules, including taurine, a sulfur- and nitrogen-rich compound involved in bile acid formation [22]. Taurine in the human body can be absorbed from the diet or synthesized in the liver [37]. However, taurine is also produced as a byproduct of the deconjugation of bile salts via bile salt hydrolases (BSHs) present in the anaerobic gut taxa *Lactobacillus* and *Clostridium* [22]. We

1059 observed increased expression of genes encoding BSH enzymes between days 12 and 86.  
 1060  
 1061 Given that increased expression of BSH genes corresponded to the beginning of active  
 1062 decomposition, when decomposition products were observed to enter the soil, and the  
 1063  
 1064 period of reduced dissolved oxygen in our study, it is likely that taurine accumulation  
 1065  
 1066 is the result of BSH enzyme activity by anaerobic microorganisms. While we did  
 1067 not measure taurine concentrations in the present study, our results correspond to  
 1068  
 1069 previous decomposition studies that report accumulation of taurine in various organs  
 1070  
 1071 and body regions [38–40] and soils [18, 41] during decomposition via metabolomics,  
 1072  
 1073 and increased relative abundance of *Clostridium* and *Lactobacillus* within the body  
 1074 [42–44] and in decomposition soils [20] via DNA sequencing methods, including in  
 1075  
 1076 these soils [13].  
 1077  
 1078 Taurine can be metabolised through desulfurization via the  $\alpha$ -ketoglutarate-dependent  
 1079  
 1080 enzyme taurine dioxygenase (TauD). Specifically, this enzyme, encoded by the gene  
 1081  
 1082 *tauD*, converts 2-oxoglutarate and taurine to produce aminoacetaldehyde, succinate,  
 1083  
 1084 sulfite, and CO<sub>2</sub> [45]. Succinate and sulfite from this reaction can then be used for  
 1085  
 1086 the citric acid cycle and sulfur metabolism, respectively. Given increased BSH expres-  
 1087  
 1088 sion in our study and reported taurine accumulation in others, we would expect  
 1089  
 1090 taurine to be present for microbial metabolism by TauD. However, we observed  
 1091  
 1092 a general decrease in *tauD* expression between days 12 through 376. This trend  
 1093  
 1094 was driven by reduced expression of *tauD* transcripts associated with *Proteobacteria*,  
 1095  
 1096 *Gammaproteobacteria*, and *Actinobacteria* whose relative abundance have been shown  
 1097  
 1098 to remain consistent or increase during human decomposition [20], suggesting that  
 1099  
 1100 *tauD* expression is downregulated under decomposition conditions. However, we noted  
 1101  
 1102 that expression of *tauD* genes associated with fungi and a few *Betaproteobacteria* dis-  
 1103  
 1104 played increased representation at day 58, corresponding to increased expression of  
 bile salt hydrolases (BSH) between days 12 and 86. The reduction in *tauD* expres-  
 sion may be due to increased sulfur availability. We did not measure sulfur species



in this experiment; however, others have observed increased sulfur concentrations in decomposition-impacted soils [3, 7, 11]. Thus, sulfur scavenging pathways such as taurine desulfurization by TauD [46], whose genes are expressed under sulfur-limiting conditions, likely display reduced expression under sulfur replete conditions. Additionally, taurine may be processed through other pathways. For example, taurine can be deaminated by taurine dehydrogenase to produce sulfite and acetyl-CoA for carbon metabolism [45, 47]. Overall, our results suggest that human decomposition has potential impacts on soil sulfur biogeochemistry through deposition of inorganic (sulfate) and organic (sulfur-containing amino acids) sulfur compounds.

## Conclusion

This study investigated soil microbial gene expression during human decomposition. Metatranscriptomic analysis of soils from three human individuals shows that decomposition impacted microbial community gene expression profiles, exhibiting functional shifts over time for over one year. This included altered expression of genes involved in lipid, N and S metabolism as microbes processed the nutrient-rich tissues of the human body. Additionally, we noted that functionality within decomposition-impacted soils was still affected after one year and had not returned to starting or background conditions. Together, these results show that vertebrate decomposition has lasting impacts on local soil ecosystems, including soil microbial communities. These results have important implications for understanding biogeochemical changes due to vertebrate mortality events in terrestrial ecosystems.

## 1151 **Materials and Methods**

1152

1153

### 1154 **Study design**

1155

1156 In February 2018, three deceased male human subjects (hereafter, “donors”) were  
1157 placed supine on the soil surface at the University of Tennessee Anthropology Research  
1158 Facility (ARF) and allowed to decompose. Located in Knoxville, TN (35° 56’ 28” N,  
1159 83° 56’ 25” W) the ARF is a roughly 2-acre outdoor facility dedicated to studying  
1160 human decomposition [48]. The soils at the ARF are comprised of the Loyston-Talbott-  
1161 Rock outcrop (LtD) and Coghill-Corryton (CcD) complexes. LtD soils are a silty clay  
1162 loam and channery clay overlaying lithic bedrock, while CcD soils are comprised of  
1163 clay from weathered quartz limestone [13, 48]. A site that had not been previously  
1164 exposed to decomposition was used for this study.

1165

1166

1167 The decomposition field experiment is fully described in Taylor et al. (2024) [13].

1168

1169 Briefly, experiments were conducted in a block design, where each block consisted of

1170

1171 one decomposition site and one control site [13]. In total three blocks, *i.e.*, three donors

1172

1173 paired with three respective control sites, were included in the study. Each control site

1174

1175 was chosen in a manner to ensure their location was uphill and roughly 2 m away from

1176

1177 decomposition sites [13]. Donor internal temperatures were recorded by probes located

1178

1179 in the abdomen, while ambient air temperatures were monitored via sensors located

1180

1181 roughly 50 cm above the soil surface. Soil temperature and salinity were measured

1182

1183 with sensors placed directly underneath each individual (Decagon Devices, GS3) [13].

1184

1185 Donor ages ranged from 65 to 86 and were within 1 kg of each other with regard to

1186

1187 weight (90.7 to 91.6 kg); donor BMI varied between 27.7 to 29.6 [13].

1188

1189

1190

1191 **Sampling and physiochemistry**

1192

1193 Decomposition of all subjects was observed for one year. During the one-year study

1194

1195 period, soils were sampled at 20 timepoints chosen to correspond with morphological

1196

stages of decomposition as described by [49]. Once advanced decay was reached, soils were collected at intervals of 350 accumulated degree days (ADD), calculated using ambient air temperatures, up to one year. All soil cores were taken using a 1.9 cm (3/4 inch) diameter soil auger to a depth of 16 cm. Soils were divided into two depth fractions: 0-1 cm (interface) and 1-16 cm (core) for the analyses reported in Taylor et al. (2024) [13]; the entire 0 to 16 cm core was used for this current study. Decomposition soils were taken from directly beneath the cadavers, taking care to not re-sample the same location more than once. At the time of sampling, soil dissolved oxygen was measured in triplicate using an Orion Star™ A329 pH/ISE/Conductivity/Dissolved Oxygen portable multiparameter meter (ThermoFisher) [13].

A subset of 6 study timepoints were chosen for metatranscriptomics analysis. Study days 0, 12, 58, 86, 168, and 376 were chosen as they represented distinct morphological and soil biogeochemical stages during decomposition. Study day 0 was chosen as a baseline sample prior to cadaver placement. Study day 12 was the start of active decomposition and corresponded to maximum soil ammonium concentrations and minimum soil oxygen (approximately 39%). Study day 58 was chosen as this sample represented the pH minimum, and respiration and soil temperature were at a maximum [13]. Additionally, ammonium concentrations began to decrease around day 58. Study day 86 was when soil oxygen started to recover and nitrate levels began to increase. Study day 168 was chosen as nitrate was at its maximum and soil dissolved oxygen had returned to 99%. Finally, day 376 was chosen to represent the end of the study, 1 year since cadaver placement. Each study day was represented by four soil samples for RNA extraction: one pooled control sample which was a mix of the three control locations, plus one sample from each of the three donors, yielding a total of 24 samples for this study.

1243 Soil samples were transported back to the University of Tennessee (Knoxville, TN)  
1244 and processed within 24 hours of collection. Soils were homogenized by hand to remove  
1245 insect larvae, roots, rocks, and other debris ( $> 2$  mm). A subset of soils were used  
1246 to measure pH, electrical conductivity (EC), and evolved  $\text{CO}_2$  as described in Taylor  
1247 (2024). Soil nitrogen species ( $\text{NH}_4^+$ ,  $\text{NO}_3^-$ ) and total carbon (TC) and nitrogen (TN)  
1248 were measured in all soil samples as described in [13]. Reported values for soil phys-  
1249 iochemistry represent the full 16 cm core; estimated by summing interface and core  
1250 values reported by Taylor et. al, (2024) [13] in 1:16 and 15:16 ratios, respectively. Con-  
1251 trol reported here are means of the three experimental controls that were unimpacted  
1252 by decomposition.

1253  
1254  
1255  
1256  
1257  
1258  
1259  
1260 Roughly 10 g of soil was reserved for nucleic acid extraction, placed in a 4 oz. Whirl-  
1261 Pak™ bag (Nasco), and flash frozen in liquid nitrogen. All samples were stored at  
1262  $-80^\circ\text{C}$  until further analysis. Bacterial and fungal community composition was assessed  
1263 via amplicon sequencing of the 16S rRNA gene and ITS2 region as described in Taylor  
1264 et al. (2024).

## 1265 1266 1267 1268 1269 1270 **RNA Extraction and Sequencing**

1271  
1272 RNA was extracted from 2 g of soil using Qiagen's RNeasy® PowerSoil® Total RNA  
1273 kit. Manufacturer's instructions were followed with a few modifications. Soils became  
1274 saline during decomposition; therefore, we followed the manufacturer's suggestion and  
1275 incubated all extracts at  $-20^\circ\text{C}$  following addition of solution SR4 (step 9) to decrease  
1276 salt precipitation. All RNA samples were resuspended in 40  $\mu\text{l}$  of Solution SR7. RNA  
1277 concentrations were assessed fluorometrically using the Qubit® RNA HS assay (cat-  
1278 alog no. Q32852) with 1  $\mu\text{l}$  of RNA. DNA contamination was removed by DNase  
1279 treating RNA extracts twice using Qiagen's DNase Max® kit in 50  $\mu\text{l}$  reactions. RNA  
1280 concentrations were remeasured after DNase treatment. PCR with V4 16S rRNA gene  
1281 primers [50, 51] was conducted using RNA extracts as the template to confirm removal

of all DNA prior to sequencing. RNA aliquots were shipped to HudsonAlpha Discovery (Huntsville, AL) for library preparation and RNA sequencing. Dual-indexed libraries were prepared using the Illumina® Stranded Total RNA prep with ribosomal RNA depletion via ligation with Ribo-Zero Plus. Libraries were then pooled and sequenced on Illumina’s NovaSeq 6000 v4 platform, resulting in demultiplexed fastq files for each sample.

## Bioinformatics

Illumina sequencing of the 24 libraries yielded a total of 5,073,476,730 reads, or 2,536,738,365 paired reads, with a mean of 105,697,432 paired reads per sample. Read quality control (QC) was conducted in KBase [52] using Trimmomatic [53]. Paired fastq files were imported to KBase through Globus. Poor quality reads were removed (4.7% of all reads), and adapters trimmed via Trimmomatic (v0.36) using default settings and the TruSeq3-PE-2 adapter file, resulting in 4,834,123,062 total reads. After QC check with FastQC, trimmed libraries were exported as fastq files from KBase through Globus. Remaining ribosomal RNA was filtered using bbmap (maxindel = 20, minid = 0.93) from the Joint Genome Institute’s (JGI) bbtools suite [54]. Filtering of ribosomal RNA further removed 7.3% of reads, leaving 4,479,804,360 reads for assembly. Following this step, all non-ribosomal reads from all 24 samples were merged into one file. Reads were then co-assembled into contigs using the de novo assembler MEGAHIT (v1.2.9) [55] (–12 –k-min 23, –k-max 123, –k-step 10).

Gene identification and annotation from co-assembled contigs was performed using Prodigal [56] and eggNOG mapper [57], respectively. Briefly, the DNA fasta containing all contigs was submitted to Prodigal (v2.6.3) for protein coding gene predication for a meta-sample (–p meta –f gff). After co-assembly, a total of 6,257,674 gene calls were identified by Prodigal. Next, predicated genes were functionally and taxonomically annotated using eggNOG mapper (v2.1.6) using basic settings to perform a

1335 diamond blastp search [58]. From this, 1,048,573 proteins were annotated by eggNOG-  
 1336 mapper (16.7%). Most of the annotated proteins were taxonomically annotated as  
 1337 bacteria (91.3%), followed by eukaryotes (7.6 %), and archaea (0.81 %). Of the 7.6%  
 1338 of eukaryotic proteins, 64.4% (4.9% of all proteins) were annotated as fungi. For this  
 1341 study, genes of interest included all bacterial, archaeal, and fungal proteins, therefore  
 1343 all non-fungal eukaryotic proteins (32,004) were removed prior to downstream analy-  
 1344 sis. Transcript counts for all genes of interest were obtained by mapping reads from  
 1346 each respective sample to genes of interest obtained from co-assembly using QIAGEN  
 1348 CLC Genomics Workbench 20.0 (<https://digitalinsights.qiagen.com/>). The percent of  
 1349 reads mapped to genes of interest ranged from 21% to 38% between samples, with an  
 1351 average of 31% reads mapped. Gene counts were then combined in a single file and  
 1352 used for downstream analyses in R.

## 1355 1356 **Differential Expression**

1358 Transcript counts from all samples were combined in a single workable data file and  
 1359 imported into R for differential expression analysis using the R packages edgeR [59]  
 1361 and limma [60] following a modified pipeline by Phipson et al. (2020) [61]. The tran-  
 1363 script count table was imported into R and converted to a DGElist object. Genes  
 1364 without sufficient counts for statistical analysis were removed to increase power using  
 1366 the edgeR function filterByExpr(), using study day as the comparison group.

1368  
 1369 Raw counts were then log2 normalized and gene expression profiles compared via  
 1370 multidimensional scaling (MDS) and hierarchical clustering. Multidimensional scaling  
 1372 (MDS) was conducted using plotMDS() from the limma package to assess differences  
 1373 between samples. MDS values were extracted from the MDS object, and the first two  
 1375 dimensions plotted using ggplot2 [62]. We also assessed the relationship between gene  
 1377 expression profiles and changes in the soil environment using canonical correspondence  
 1378 analysis (CCA). Environmental variables of interest included decomposition time in  
 1380

accumulated degree hours (ADH) based on ambient temperatures, ADH based on  
 internal gut temperatures, ADH based on soil temperatures, gravimetric moisture,  
 pH, electrical conductivity (EC), dissolved oxygen (DO),  $\text{CO}_2$  ( $\mu\text{mol gdw}^{-1}$ ),  $\text{NH}_4$  (mg  
 $\text{gdw}^{-1}$ ),  $\text{NO}_3$  (mg  $\text{gdw}^{-1}$ ), N %, C %, and CN ratio. First, permutational multivariate  
 analysis of variance (PERMANOVA) with `adonis()` (vegan v2.6.7) [63] was used to  
 identify significant soil parameters. Then the vegan functions `cca()` and `scores()` were  
 applied to run the CCA and extract scores, respectively. Scores for the first two  
 dimension were plotted using `ggplot2`, with loadings extracted from the CCA biplot.  
 For differential expression analysis, raw filtered reads were normalized using edgeR's  
 trimmed mean of M values (TMM) normalization using the function `calcNormFac-`  
`tors()`. TMM normalized reads were then log2 transformed using limma's `voom()` and  
 differential expression assessed. Empirical Bayes shrinkage was used correct to p-  
 values for false discovery rates. The topmost up and down regulated genes for each  
 comparison, determined by log2 fold change and adjusted p-values, were then reported.  
 Expression of certain genes were assessed after performing transcripts per million  
 (TPM) normalization and statistical analyses with a combination of analysis of vari-  
 ance (ANOVA) and post-hoc Tukey tests. ANOVA across all timepoints were applied  
 to hierarchical linear mixed effects models to account for repeated sampling within  
 each donor block.

## Data availability

Raw RNA sequence files from the Illumina Novaseq are available at the National Cen-  
 ter for Biotechnology Information's (NCBI) Sequence Read Archive (SRA) as a part  
 of [BioProject PRJNA1066312](#) under BioSample accession numbers SAMN45195141-  
 SAMN45195164. Additional datasets supporting the conclusions of this article are  
 available on [GitHub](#).

## 1427 Code availability

1428

1429 The code used for analysis and to generate figures are available on [GitHub](#).

1430

1431

## 1432 References

1433

1434

1435 [1] Benninger, L. A., Carter, D. O. & Forbes, S. L. The biochemical alteration of soil  
1436 beneath a decomposing carcass. *Forensic Science International* **180**, 70–5 (2008).

1437

1438  
1439 [2] Towne, E. G. Prairie vegetation and soil nutrient responses to ungulate carcasses.  
1440 *Oecologia* **122**, 232–239 (2000). URL <https://doi.org/10.1007/PL00008851>.

1441

1442  
1443 [3] DeBruyn, J. M., Keenan, S. W. & Taylor, L. S. From carrion to soil: microbial  
1444 recycling of animal carcasses. *Trends in Microbiology* (2024). URL <https://doi.org/10.1016/j.tim.2024.09.003>. Publisher: Elsevier.

1445

1446  
1447 [4] Parmenter, R. R. & MacMahon, J. A. Carrion decomposition and nutrient cycling  
1448 in a semiarid shrub–steppe ecosystem. *Ecological Monographs* **79**, 637–661 (2009).

1449

1450  
1451 [5] Macdonald, B. C. T. *et al.* Carrion decomposition causes large and lasting effects  
1452 on soil amino acid and peptide flux. *Soil Biology and Biochemistry* **69**, 132–140  
1453 (2014).

1454

1455  
1456 [6] Bump, J. K. *et al.* Ungulate carcasses perforate ecological filters and create  
1457 biogeochemical hotspots in forest herbaceous layers allowing trees a competitive  
1458 advantage. *Ecosystems* **12**, 996–1007 (2009).

1459

1460  
1461 [7] Aitkenhead-Peterson, J. A., Owings, C. G., Alexander, M. B., Larison, N. &  
1462 Bytheway, J. A. Mapping the lateral extent of human cadaver decomposition  
1463 with soil chemistry. *Forensic Science International* **216**, 127–34 (2012).

1464

1465

1466

1467

1468

1469

1470

1471

1472



- [8] Keenan, S. W., Schaeffer, S. M., Jin, V. L. & DeBruyn, J. M. Mortality hotspots: 1473  
nitrogen cycling in forest soils during vertebrate decomposition. *Soil Biology and* 1474  
*Biochemistry* **121**, 165–176 (2018). 1475  
1476  
1477  
1478
- [9] Fancher, J. P. *et al.* An evaluation of soil chemistry in human cadaver decom- 1479  
position islands: Potential for estimating postmortem interval (PMI). *Forensic* 1480  
*Science International* **279**, 130–139 (2017). 1481  
1482  
1483  
1484
- [10] Quaggiotto, M.-M., Evans, M. J., Higgins, A., Strong, C. & Barton, P. S. 1485  
Dynamic soil nutrient and moisture changes under decomposing vertebrate 1486  
carcasses. *Biogeochemistry* **146**, 71–82 (2019). 1487  
1488  
1489
- [11] Taylor, L. S. *et al.* Soil elemental changes during human decomposition. 1490  
*PLoS ONE* **18**, 1–24 (2023). URL <https://doi.org/10.1371/journal.pone.0287094>. 1491  
1492  
1493  
Publisher: Public Library of Science. 1494  
1495
- [12] Mason, A. R. *et al.* Body mass index (BMI) impacts soil chemical and microbial 1496  
response to human decomposition. *mSphere* e0032522 (2022). 1497  
1498  
1499
- [13] Taylor, L. S. *et al.* Transient hypoxia drives soil microbial community dynamics 1500  
and biogeochemistry during human decomposition. *FEMS Microbiology Ecology* 1501  
**100**, fae119 (2024). URL <https://doi.org/10.1093/femsec/fae119>. 1502  
1503  
1504  
1505
- [14] Keenan, S. W., Emmons, A. L. & DeBruyn, J. M. Microbial community coa- 1506  
lescence and nitrogen cycling in simulated mortality decomposition hotspots. 1507  
*Ecological Processes* **12**, 45 (2023). URL [https://doi.org/10.1186/s13717-023-](https://doi.org/10.1186/s13717-023-00451-y) 1508  
[00451-y](https://doi.org/10.1186/s13717-023-00451-y). 1509  
1510  
1511  
1512  
1513
- [15] Mason, A. R., Taylor, L. S. & DeBruyn, J. M. Microbial ecology of vertebrate 1514  
decomposition in terrestrial ecosystems. *FEMS Microbiology Ecology* **99**, fiad006 1515  
(2023). URL <https://doi.org/10.1093/femsec/fiad006>. 1516  
1517  
1518

1519 [16] Burcham, Z. M. *et al.* Total RNA analysis of bacterial community structural  
1520 and functional shifts throughout vertebrate decomposition. *Journal of Forensic*  
1521 *Sciences* **64**, 1707–1719 (2019).  
1522  
1523  
1524  
1525 [17] Ashe, E. C., Comeau, A. M., Zejdlik, K. & O’Connell, S. P. Characterization of  
1526 bacterial community dynamics of the human mouth throughout decomposition  
1527 via metagenomic, metatranscriptomic, and culturing techniques. *Frontiers in*  
1528 *Microbiology* **12**, 689493 (2021).  
1529  
1530  
1531  
1532 [18] DeBruyn, J. M. *et al.* Comparative decomposition of humans and pigs: soil biogeo-  
1533 chemistry, microbial activity and metabolomic profiles. *Frontiers in Microbiology*  
1534 **11**, 608856 (2021).  
1535  
1536  
1537  
1538 [19] Howard, G. T., Duos, B. & Watson-Horzelski, E. J. Characterization of the  
1539 soil microbial community associated with the decomposition of a swine carcass.  
1540 *International Biodeterioration & Biodegradation* **64**, 300–304 (2010).  
1541  
1542  
1543  
1544 [20] Cobaugh, K. L., Schaeffer, S. M. & DeBruyn, J. M. Functional and structural  
1545 succession of soil microbial communities below decomposing human cadavers.  
1546 *Plos One* **10**, e0130201 (2015).  
1547  
1548  
1549  
1550 [21] Singh, B. *et al.* Temporal and spatial impact of human cadaver decomposition  
1551 on soil bacterial and arthropod community structure and function. *Frontiers in*  
1552 *Microbiology* **8**, 2616 (2018).  
1553  
1554  
1555  
1556 [22] Urdaneta, V. & Casadesús, J. Interactions between Bacteria and Bile Salts in  
1557 the Gastrointestinal and Hepatobiliary Tracts. *Frontiers in Medicine* **4** (2017).  
1558  
1559  
1560 [23] van der Wal, A., Geydan, T. D., Kuyper, T. W. & de Boer, W. A thready affair:  
1561 linking fungal diversity and community dynamics to terrestrial decomposition  
1562 processes. *FEMS Microbiology Reviews* **37**, 477–494 (2013).  
1563  
1564

- [24] Essington, M. E. *Soil and water chemistry: an integrative approach* (CRC press, 2015). 1565  
1566  
1567  
1568
- [25] Peng, J., Wegner, C.-E. & Liesack, W. Short-term exposure of paddy soil microbial communities to salt stress triggers different transcriptional responses of key taxonomic groups. *Frontiers in Microbiology* **8** (2017). 1569  
1570  
1571  
1572  
1573  
1574
- [26] Pandit, A. S. *et al.* A snapshot of microbial communities from the Kutch: one of the largest salt deserts in the World. *Extremophiles* **19**, 973–987 (2015). 1575  
1576  
1577  
1578
- [27] Metcalf, J. L. *et al.* Microbial community assembly and metabolic function during mammalian corpse decomposition. *Science* **351**, 158–62 (2016). 1579  
1580  
1581  
1582
- [28] Fu, X. *et al.* Fungal succession during mammalian cadaver decomposition and potential forensic implications. *Scientific Reports* **9**, 12907 (2019). 1583  
1584  
1585  
1586
- [29] Dujon, B. *et al.* Genome evolution in yeasts. *Nature* **430**, 35–44 (2004). 1587  
1588  
1589
- [30] Haridas, S. *et al.* The genome and transcriptome of the pine saprophyte *Ophiostoma piceae*, and a comparison with the bark beetle-associated pine pathogen *Grosmannia clavigera*. *BMC Genomics* **14**, 373 (2013). 1590  
1591  
1592  
1593  
1594  
1595
- [31] Notter, S. J., Stuart, B. H., Rowe, R. & Langlois, N. The initial changes of fat deposits during the decomposition of human and pig remains. *Journal of Forensic Sciences* **54**, 195–201 (2009). 1596  
1597  
1598  
1599  
1600  
1601
- [32] Kok, R. G. *et al.* Characterization of the extracellular lipase, LipA, of *Acinetobacter calcoaceticus* BD413 and sequence analysis of the cloned structural gene. *Molecular Microbiology* **15**, 803–818 (1995). 1602  
1603  
1604  
1605  
1606  
1607
- [33] Hasan, F., Shah, A. A. & Hameed, A. Influence of culture conditions on lipase production by *Bacillus* sp. FH5. *Annals of Microbiology* **56**, 247–252 (2006). 1608  
1609  
1610

1611 [34] Zouaoui, B. & Bouziane, A. Production, optimization and characterization of  
1612 the lipase from *Pseudomonas aeruginosa*. *Romanian biotechnological letters* **17**,  
1613 7187–7193 (2012).  
1614  
1615  
1616  
1617 [35] Soler-Jofra, A., Pérez, J. & van Loosdrecht, M. C. M. Hydroxylamine and the  
1618 nitrogen cycle: A review. *Water Research* **190**, 116723 (2021).  
1619  
1620  
1621 [36] Yu, R., Perez-Garcia, O., Lu, H. & Chandran, K. Nitrosomonas europaea adapta-  
1622 tion to anoxic-oxic cycling: Insights from transcription analysis, proteomics and  
1623 metabolic network modeling. *Science of the Total Environment* **615**, 1566–1573  
1624 (2018).  
1625  
1626  
1627  
1628 [37] Seidel, U., Huebbe, P. & Rimbach, G. Taurine: A regulator of cellular redox  
1629 homeostasis and skeletal muscle function. *Molecular Nutrition & Food Research*  
1630 **63**, 1800569 (2019).  
1631  
1632  
1633  
1634 [38] Mora-Ortiz, M., Trichard, M., Oregioni, A. & Claus, S. P. Thanatometabolomics:  
1635 introducing NMR-based metabolomics to identify metabolic biomarkers of the  
1636 time of death. *Metabolomics* **15**, 37 (2019).  
1637  
1638  
1639  
1640 [39] Locci, E. *et al.* A <sup>1</sup>H NMR metabolomic approach for the estimation of the time  
1641 since death using aqueous humour: an animal model. *Metabolomics* **15**, 76 (2019).  
1642  
1643  
1644 [40] Zelentsova, E. A. *et al.* Post-mortem changes in the metabolomic compositions  
1645 of rabbit blood, aqueous and vitreous humors. *Metabolomics* **12**, 172 (2016).  
1646  
1647  
1648 [41] Hoeland Katharina, M. *Investigating the potential of postmortem metabolomics*  
1649 *in mammalian decomposition studies in outdoor settings*. Ph.D. thesis, University  
1650 of Tennessee-Knoxville, [https://trace.tennessee.edu/utk\\_graddiss/7000](https://trace.tennessee.edu/utk_graddiss/7000) (2021).  
1651  
1652  
1653  
1654  
1655  
1656

- [42] Javan, G. T. *et al.* Human thanatomicrobiome succession and time since death. *Scientific Reports* **6**, 29598 (2016). 1657  
1658  
1659  
1660
- [43] Javan, G. T., Finley, S. J., Smith, T., Miller, J. & Wilkinson, J. E. Cadaver 1661  
thanatomicrobiome signatures: the ubiquitous nature of *Clostridium* species in 1662  
human decomposition. *Frontiers in Microbiology* **8**, 2096 (2017). 1663  
1664  
1665  
1666
- [44] DeBruyn, J. M. & Hauther, K. A. Postmortem succession of gut microbial 1667  
communities in deceased human subjects. *Peerj* **5**, e3437 (2017). 1668  
1669  
1670
- [45] Cook, A. M. & Denger, K. Metabolism of taurine in microorganisms. *Taurine* **6** 1671  
3–13 (2006). 1672  
1673  
1674
- [46] Kertesz, M. A. Riding the sulfur cycle – metabolism of sulfonates and sul- 1675  
fate esters in Gram-negative bacteria. *FEMS Microbiology Reviews* **24**, 135–175 1676  
(2000). 1677  
1678  
1679  
1680
- [47] Brüggemann, C., Denger, K., Cook, A. M. & Ruff, J. Enzymes and genes of 1681  
taurine and isethionate dissimilation in *Paracoccus denitrificans*. *Microbiology* 1682  
(Reading, England) **150**, 805–816 (2004). 1683  
1684  
1685  
1686
- [48] Keenan, S. W. *et al.* Spatial impacts of a multi-individual grave on microbial 1687  
and microfaunal communities and soil biogeochemistry. *PLoS One* **13**, e0208845 1688  
(2018). 1689  
1690  
1691  
1692
- [49] Payne, J. A. A summer carrion study of the baby pig *Sus Scrofa* Linnaeus. 1693  
*Ecology* **46**, 592–602 (1965). 1694  
1695  
1696
- [50] Apprill, A., McNally, S., Parsons, R. & Weber, L. Minor revision to V4 region SSU 1697  
rRNA 806R gene primer greatly increases detection of SAR11 bacterioplankton. 1698  
*Aquatic Microbial Ecology* **75**, 129–137 (2015). 1699  
1700  
1701  
1702

1703 [51] Parada, A. E., Needham, D. M. & Fuhrman, J. A. Every base matters: assessing  
1704 small subunit rRNA primers for marine microbiomes with mock communities,  
1705 time series and global field samples. *Environmental Microbiology* **18**, 1403–14  
1706 (2016).  
1707  
1708  
1709  
1710 [52] Arkin, A. P. *et al.* KBase: The United States Department of Energy Systems  
1711 Biology Knowledgebase. *Nature Biotechnology* **36**, 566–569 (2018).  
1712  
1713  
1714 [53] Bolger, A. M., Lohse, M. & Usadel, B. Trimmomatic: a flexible trimmer for  
1715 Illumina sequence data. *Bioinformatics* **30**, 2114–2120 (2014).  
1716  
1717  
1718  
1719 [54] Bushnell, B. Bbtools software packag. *e* (2014).  
1720  
1721 [55] Li, D., Liu, C.-M., Luo, R., Sadakane, K. & Lam, T.-W. MEGAHIT: an ultra-fast  
1722 single-node solution for large and complex metagenomics assembly via succinct  
1723 de Bruijn graph. *Bioinformatics* **31**, 1674–1676 (2015).  
1724  
1725  
1726  
1727 [56] Hyatt, D. *et al.* Prodigal: prokaryotic gene recognition and translation initiation  
1728 site identification. *BMC Bioinformatics* **11**, 119 (2010).  
1729  
1730  
1731 [57] Cantalapiedra, C. P., Hernández-Plaza, A., Letunic, I., Bork, P. & Huerta-  
1732 Cepas, J. eggNOG-mapper v2: functional annotation, orthology assignments, and  
1733 domain prediction at the metagenomic scale. *Molecular Biology and Evolution*  
1734 **38**, 5825–5829 (2021).  
1735  
1736  
1737  
1738 [58] Buchfink, B., Reuter, K. & Drost, H.-G. Sensitive protein alignments at tree-of-  
1739 life scale using DIAMOND. *Nature Methods* **18**, 366–368 (2021).  
1740  
1741  
1742 [59] Robinson, M. D., McCarthy, D. J. & Smyth, G. K. edgeR: a Bioconduc-  
1743 tor package for differential expression analysis of digital gene expression data.  
1744 *Bioinformatics* **26**, 139–140 (2010).  
1745  
1746  
1747  
1748

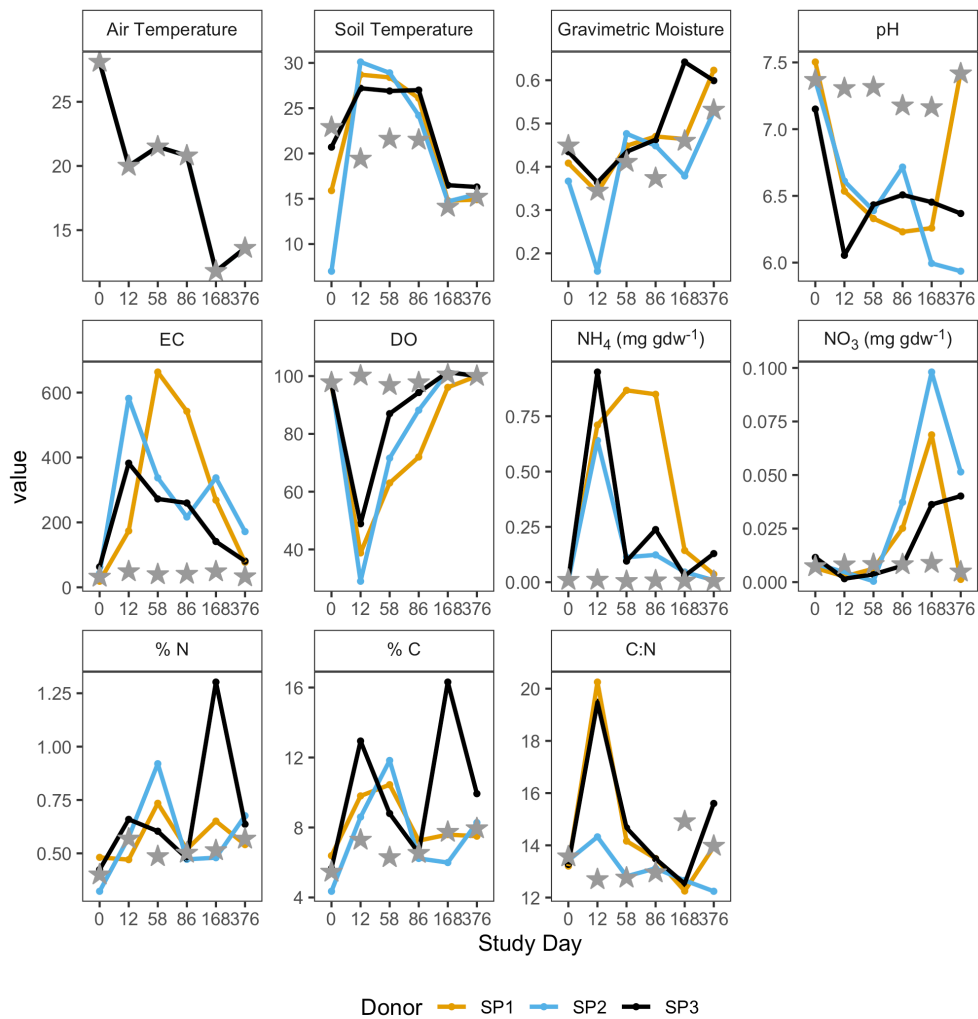
- [60] Smyth, G. K. in *limma: Linear Models for Microarray Data* (eds Gentleman, R., Carey, V. J., Huber, W., Irizarry, R. A. & Dudoit, S.) *Bioinformatics and Computational Biology Solutions Using R and Bioconductor* 397–420 (Springer New York, New York, NY, 2005).
- [61] Phipson, B. *et al.* Differential expression analysis (2020). URL <https://combine-australia.github.io/RNAseq-R/06-rnaseq-day1.html#References>.
- [62] Wickham, H. *ggplot2: Elegant Graphics for Data Analysis* (Springer-Verlag New York, 2016). URL <https://ggplot2.tidyverse.org>.
- [63] Oksanen, J. *et al.* *vegan: Community Ecology Package* (2024). URL <https://vegandevs.github.io/vegan/>.

## Acknowledgements

We would like to thank the Forensic Anthropology Center at the University of Tennessee-Knoxville for their help in setting up field experiments. We would like to thank Mary Davis for her help in managing the field site and helping to obtain donors for this work. This research was funded by a National Institute of Justice Award (DOJ-NIJ-2017-R2-CX-0008) to LST and JMD.

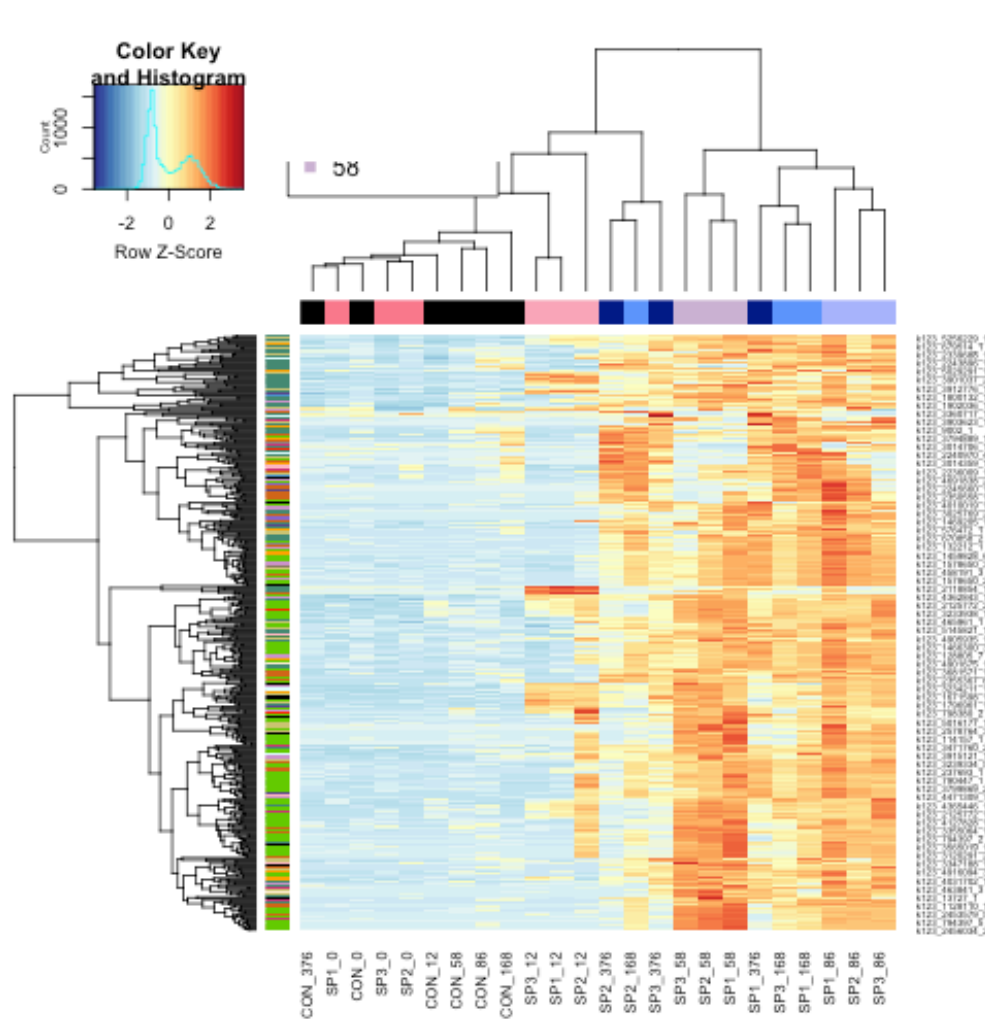
## Supplementary Information

1795  
 1796  
 1797  
 1798  
 1799  
 1800  
 1801  
 1802  
 1803  
 1804  
 1805  
 1806  
 1807  
 1808  
 1809  
 1810  
 1811  
 1812  
 1813  
 1814  
 1815  
 1816  
 1817  
 1818  
 1819  
 1820  
 1821  
 1822  
 1823  
 1824  
 1825  
 1826  
 1827  
 1828  
 1829  
 1830  
 1831  
 1832  
 1833  
 1834  
 1835  
 1836  
 1837  
 1838  
 1839  
 1840



Supplementary Material 1: Figure S1. Soil physiochemical parameters in decomposition soils during the one-year study. Data is shown for each individual donor: SP1 (gold), SP2 (blue), and SP2 (black). Values for the full 16 cm core samples were estimated by summing values interface (0-1 cm) and core (0-16 cm) reported by Taylor et al, (2024) in 1:16 and 15:16 ratios, respectively. Controls reported here are means of three experimental controls that were unimpacted by decomposition and are represented by stars.



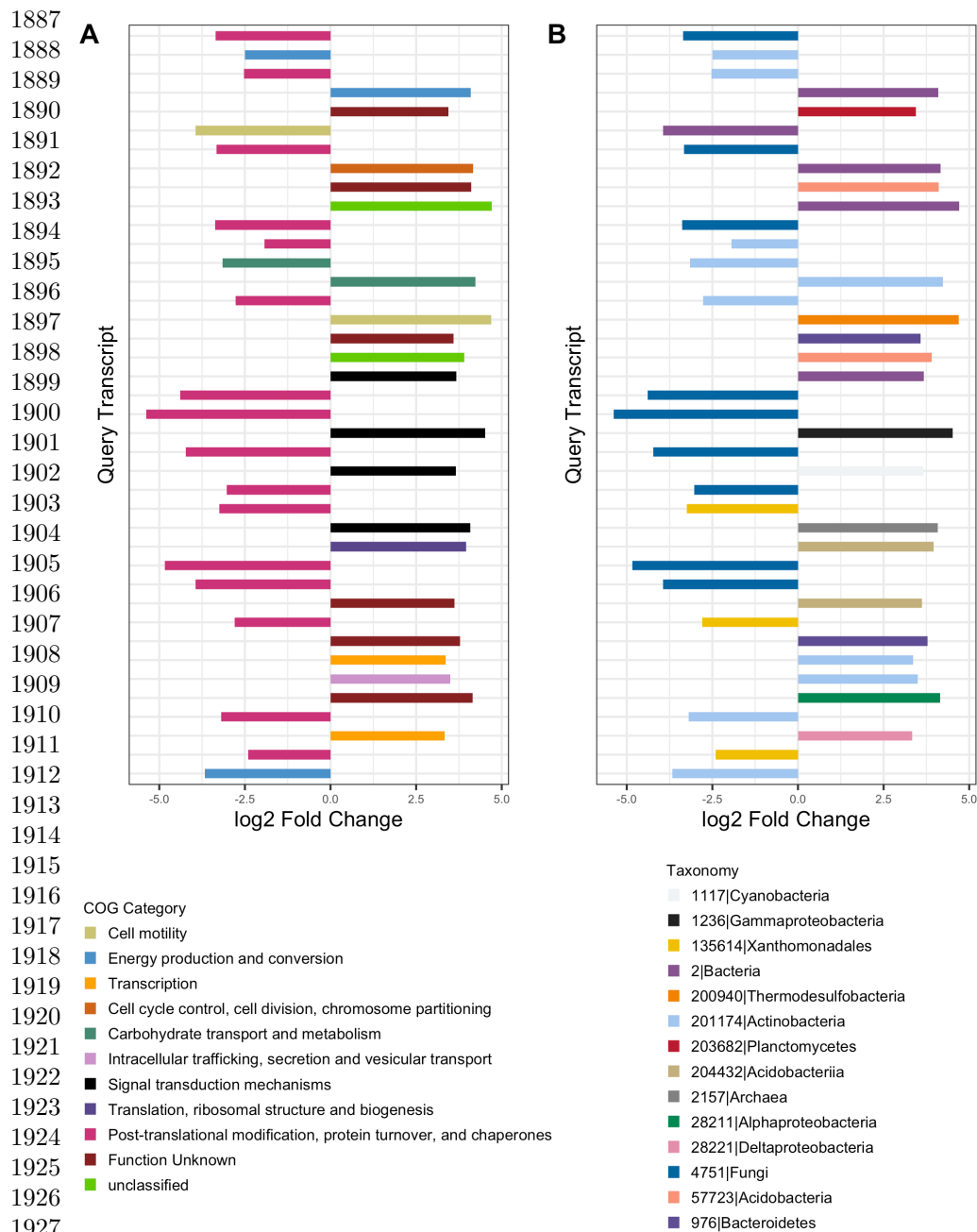


Supplementary Material 2: Figure S2. Hierarchical clustering heatmap showing the log counts per million (CPM) of the top 500 most variable genes across samples. Variable genes were determined by selecting genes with the highest variance in gene expression. Samples are clustered along the x-axis using Euclidean distances between samples and colored by study day.

Table S1. Permutational analysis of variance (PERMANOVA) results identifying significant environmental parameters which explain some of the variation in soil gene expression profiles. Environmental parameter data is from Taylor et al. (2024).

Variables with  $p < 0.05$  are indicated in bold.

Supplementary Material 3



Supplementary Material 4: Figure S3. Top 40 up- and down-regulated genes in controls relative to decomposition soils across all study days, colored by COG functional category (A) and taxonomic annotation (B). Positive values denote higher expression in controls, while negative values are higher in decomposition soils.

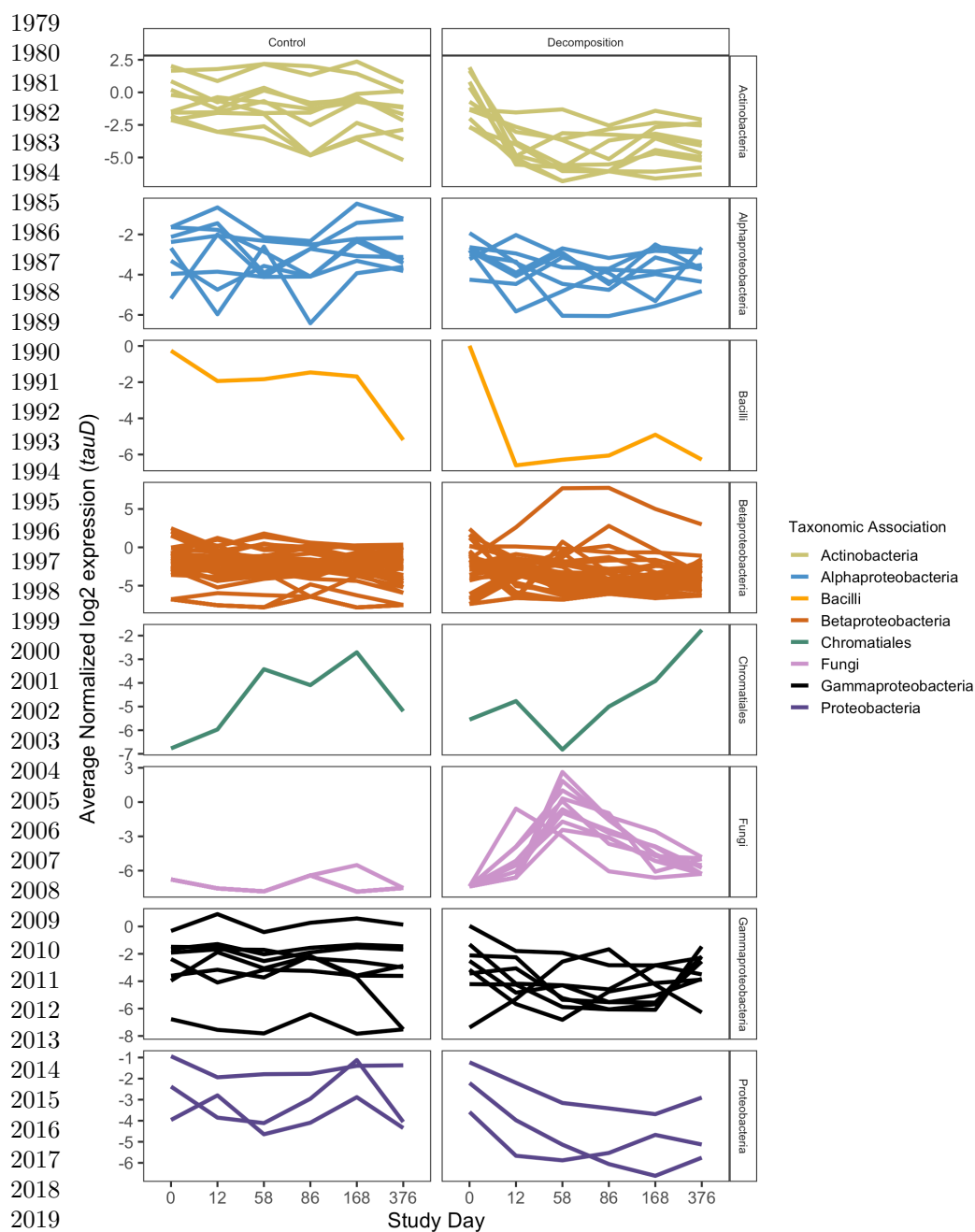
Table S2. Top 20 most up- and down-regulated gene queries, determined by log2 fold change and adjusted p-values, in control relative to decomposition soils. Positive log2 fold change values represent genes whose expression was higher in control soils, while negative log2 fold change values were higher in decomposition soils. Taxonomic annotation, COG categories, gene description, gene names, and EC were assigned via eggNOG-mapper.

Supplementary Material 5

Table S3. Top 10 most up- and down-regulated genes, determined by log2 fold change and adjusted p-values, for each sequential timepoint comparison. Positive log2 fold change values represent genes whose expression was higher in the later decomposition timepoint soils, while negative log2 fold change values are higher in earlier decomposition timepoint soils. Taxonomic annotation, COG categories, gene names, and EC were assigned via eggNOG-mapper. The comparison column distinguishes each timepoint comparison.

Supplementary Material 6

1933  
1934  
1935  
1936  
1937  
1938  
1939  
1940  
1941  
1942  
1943  
1944  
1945  
1946  
1947  
1948  
1949  
1950  
1951  
1952  
1953  
1954  
1955  
1956  
1957  
1958  
1959  
1960  
1961  
1962  
1963  
1964  
1965  
1966  
1967  
1968  
1969  
1970  
1971  
1972  
1973  
1974  
1975  
1976  
1977  
1978



Supplementary Material 7: Figure S4. Mean normalized log<sub>2</sub> expression of *tauD* genes by taxonomic association (color) in control and decomposition soils at each study day. Each line represents one *tauD* gene query, while color denotes taxonomic association as determined by eggNOG-mapper.